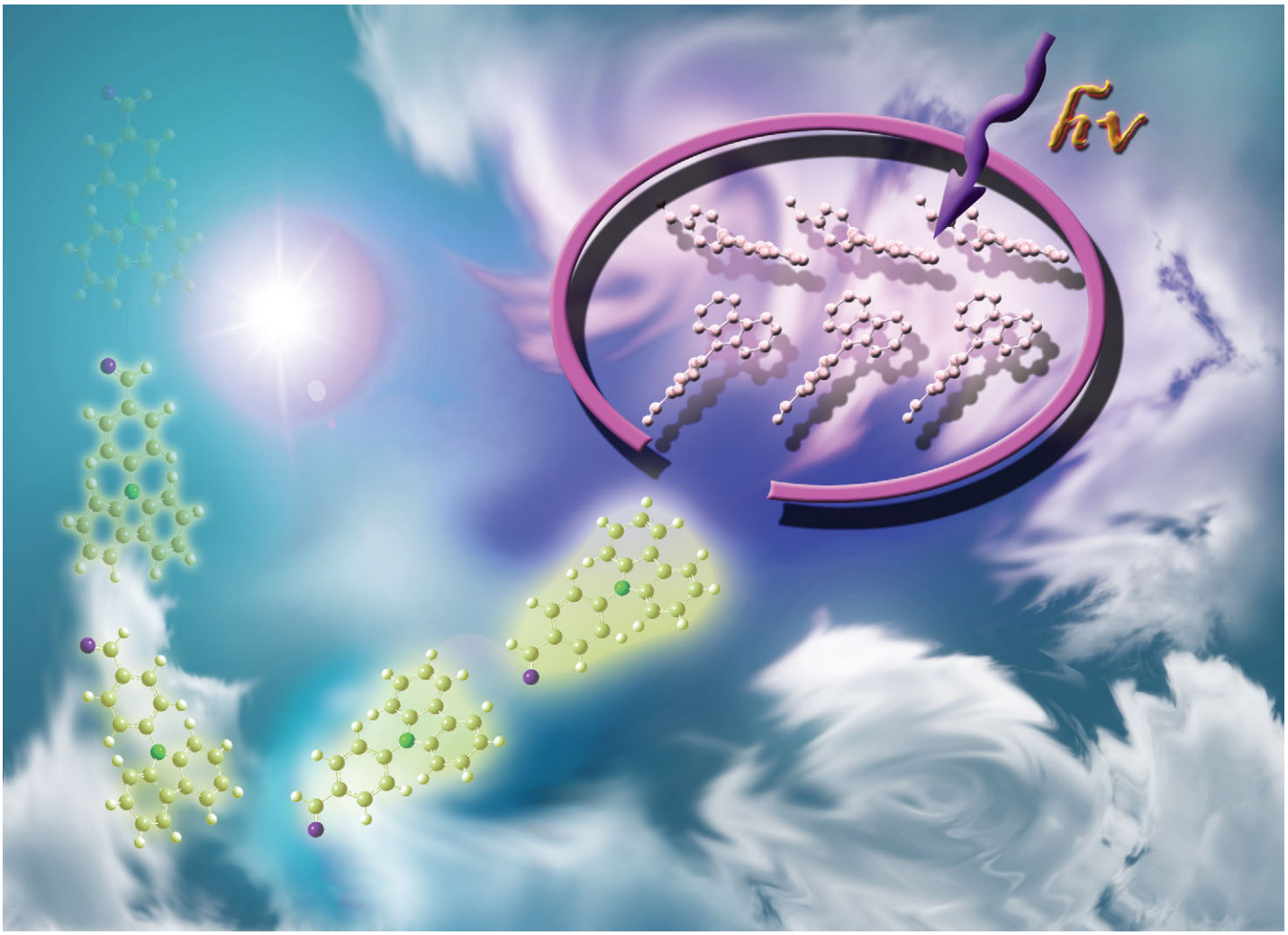

Showcasing research from Pengchong Xue's Laboratory, College of Chemistry, Jilin University, China

Luminescence switching of a persistent room-temperature phosphorescent pure organic molecule in response to external stimuli

A metal- and heavy atom-free organic molecule exhibits persistent room-temperature phosphorescence and a multicolour phosphorescence-to-fluorescence switching property in response to mechanical force stimuli.

As featured in:

See Pengchong Xue *et al.*, *Chem. Commun.*, 2015, **51**, 10381.

ROYAL SOCIETY OF CHEMISTRY

www.rsc.org/chemcomm

Registered charity number: 207890

ChemComm

COMMUNICATION

View Article Online
View Journal | View Issue

Cite this: *Chem. Commun.*, 2015, **51**, 10381

Received 29th April 2015,
Accepted 19th May 2015

DOI: 10.1039/c5cc03403e

www.rsc.org/chemcomm

Luminescence switching of a persistent room-temperature phosphorescent pure organic molecule in response to external stimuli†

Pengchong Xue,*[a] Jiabao Sun,[a] Peng Chen,[b] Panpan Wang,[a] Boqi Yao,[a] Peng Gong,[a] Zhenqi Zhang[a] and Ran Lu[a]

4-(Carbazol-9-yl)benzaldehyde could emit yellow RTP, which could last for 3 s because of efficient intersystem crossing. Moreover, multicolor luminescent switches could be realized by simply applying a mechanical force stimulus.

Smart luminescent materials that are responsive to external stimuli have received considerable interest. Especially, mechanochromic emissive organic π-conjugated molecules recently have received increasing attention both in the fundamental research field and in the applied field.[1] These luminescent organic molecules can show changes in their emissive color under mechanical stress because the molecular packing model in the solid state is generally changed under a pressure stimulus. Among them, fluorescence is the main emissive type, and only metal complexes with short phosphorescence lifetimes (<1 ms) have been found to exhibit mechanochromic behaviour[2] because prolonged room-temperature phosphorescence (RTP) of pure or metal-free organic molecules is still difficult considering that their long-lived triplet states are prone to internal or external quenching.

According to El-Sayed's rule, spin–orbital coupling is forbidden between states of the same configuration.[3] Therefore, the rate constants of the transition from[3] (n,π*) to the ground state are always larger than those of the transition from[3] (π,π*) to the ground state.[4] This mechanism provides an opportunity to find organic molecules that exhibit persistent RTP if their lowest lying triplet states are assigned as[3] (π,π*) states. Kearns and Itoh implied that some acetophenone and benzaldehyde derivatives such as 4-methoxyl acetophenone, 4-hydroxyl acetophenone, *N*-(4-butyrylphenyl)acetamide, and 4-methoxybenzaldehyde possess the lowest triplet state of π,π* character.[5] It was also revealed that the phosphorescence lifetimes of these derivatives are long, ranging from 60 ms to 1 s at 77 K. This result indicates that 4-position-substituted electron-donating groups may cause benzaldehyde derivatives to have a T_1 state with π,π* character and then increase the chance of achieving persistent RTP materials.

Numerous studies have suggested that nonplanar D–π–A π-conjugated molecules always contribute to the realization of fluorescence change under pressure.[6] Herein, a carbazole moiety was introduced into a benzaldehyde matrix to prepare a D–π–A and nonplanar π-conjugated molecule (**CBA**, Scheme 1), in which a formyl moiety served as a functional group to generate an intrinsic triplet state through intersystem crossing (ISC) because of a degree of spin–orbit coupling at the carbonyl oxygen. Then, a carbazole unit was used as an electron-donating unit that allows the lowest π,π* triplet state. As expected, in crystal and powder states, it showed a persistent yellow RTP with a lifetime of 540 ms. Moreover, reversible conversion from phosphorescence to fluorescence was realized through mechanical force. **CBA** is the first pure organic material (*i.e.*, without metal, other heavy atoms, or host) to exhibit persistent RTP and respond to external force. It is believed that such simple and low-cost organic molecules will be excellent candidates in the anti-counterfeiting field.

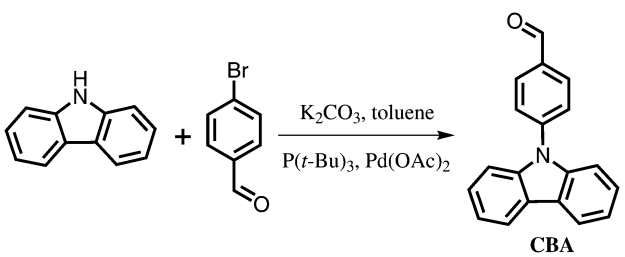

Scheme 1

[a] *State Key Laboratory of Supramolecular Structure and Materials, College of Chemistry, Jilin University, 2699 Qianjin Street, Changchun, P. R. China. E-mail: xuepengchong@jlu.edu.cn, luran@mail.jlu.edu.cn*

[b] *Key Laboratory of Functional Inorganic Material Chemistry (MOE), Chemistry and Materials Science, Heilongjiang University, No. 74, Xuefu Road, Nangang District, Harbin, P. R. China*

† Electronic supplementary information (ESI) available: A video about persistent RTP, crystal data cif file, NMR spectra, tables of photophysical data, stimulated transitions in solvents and crystals, and energy levels of frontier orbitals, UV-vis absorption and fluorescence spectra in different solvents, frontier orbitals, XRD patterns, fluorescence spectra of **CBA** in DMSO at different temperatures, and emissive decay curves of crystals and ground samples. CCDC 1037574. For ESI and crystallographic data in CIF or other electronic format see DOI: 10.1039/c5cc03403e

This compound was synthesized *via* a one-step reaction, as shown in Scheme 1. It was fully characterized by ^{1}H and ^{13}C NMR spectroscopy (Fig. S1 and S2, ESI†) and elemental analysis, and further confirmed by single-crystal X-ray diffraction (XRD) analysis. The absorption band of **CBA** in cyclohexane demonstrated good vibrational structure with three absorption peaks at 324, 339, and 355 nm (Fig. S3a, ESI†). The optical energy band gap (E_g) of **CBA** was calculated to be 3.38 eV from the onset of absorption (367 nm).[7] Similar absorption peaks with slight red shifts were observed in other solvents, and the vibrational structure of the absorption band became poor. The maximal emission peak was located at 376 nm in cyclohexane (Table S1, ESI†); thus, its singlet state (S_1) was estimated to be 3.30 eV. An increase in solvent polarity caused a continuous red shift of the emission band (Fig. S3b, ESI†), indicating that the absorption and emission bands in different solvents can be ascribed to twisted intramolecular charge transfer (TICT) transition because the carbazole and formyl moieties may act as electron-donating and electron-withdrawing groups, respectively, and a linear relationship between emission energy and solvent polarity can be expected in cyclohexane (Fig. S3c, ESI†).[8] The temperature-dependent fluorescence spectra in DMSO further confirmed this TICT emission (Fig. S4, ESI†). When the temperature was decreased to 0 °C, the liquid DMSO solution became a transparent solid, the emissive peak at 376 nm from the locally excited state became strong, and the peak at 508 nm from the solvent relaxed state became relatively weak.[9] The stimulated absorption spectrum in cyclohexane exhibited a strong absorption band at 388.7 nm and could be attributed to the HOMO → LUMO transition (Table S2, ESI†). The HOMO was mainly distributed at the carbazole unit and ascribed to the π orbital, whereas the π* orbital of benzaldehyde was principally attributed to the LUMO (Fig. S5a, ESI†). This result also implies that the S_1 state is an ICT state and holds the π,π* configuration.

When we measured the fluorescence quantum yield, it was found that **CBA** in CH_2Cl_2 and DMF had stronger fluorescence, but emitted very weak fluorescence in other solvents (Table S1, ESI†). In general, the ICT molecules have strong fluorescence in nonpolar solvents and emit weak fluorescence in polar solvents.[10] The efficiency of ISC in aromatic carbonyl compounds is high.[11] Therefore, such an abnormal change in quantum yields in different solvents may be caused by the difference in ISC. To provide insights into this difference, a series of quantum chemical calculations was carried out. The lowest triplet state (T_1) can be mainly ascribed to the π–π* transition (Table S2, ESI†) in cyclohexane and CH_2Cl_2. Two high triplet states (T_2 and T_3) were observed between S_1 and T_1 in cyclohexane, T_2 can be attributed to the transition from HOMO-3 to LUMO, meaning a T_{n,π^*} state and T_3 also contained n,π* configurations. The ISC between an S_{π,π^*} state and a low-lying T_{n,π^*} state was very rapid; thus, the emission in cyclohexane was weak (Fig. S5b, ESI†). In polar CH_2Cl_2, T_2, a π,π* state, slightly increased in state energy; however, the state energy of T_3, an n,π* state, obviously increased and lay above the lowest singlet state because of the energy decrease in the n orbital (Table S3, ESI†). This phenomenon prevented the efficient ISC from the S_1 to T_3 state. Hence, strong emission appeared in polar CH_2Cl_2. The decrease of fluorescence quantum yield in stronger polar solvents (DMSO, ethanol, and acetonitrile) originated from solvent relaxation, which increased the nonradiative deactivation of the excited molecules.[12]

As discussed above, the weak luminescence in cyclohexane can be ascribed to the efficient ISC, and then phosphorescence can be expected. However, the N_2-saturated cyclohexane solution did not exhibit phosphorescence at room temperature probably because of the rapid nonradiative decay of the long-lived triplet state caused by intramolecular motion, vibrational relaxing, and solute–solvent collisions.[6a] A strong blue luminescence (λ_{em} = 454 nm) of the frozen cyclohexane solution at 77 K was observed (Fig. 1a). After UV light was removed; the frozen solid still emitted blue light and lasted less than 1 s, indicating phosphorescence. The lifetime was as long as 95 ms. From the emission wavelength, the triplet energy (T_1) of the compound was determined to be 2.73 eV. This relatively long lifetime also confirmed the success of the design. This result also implies that the suppression of molecular motion promotes phosphorescence activation.[13] An RTP with a long lifetime is anticipated to be visible to the naked eye.

As expected, the as-synthesized solid emitted pink luminescence under 365 nm light. When the light was turned off, a persistent yellow emission was observed. To further investigate the RTP of **CBA**, its crystals were prepared by slow solvent evaporation in *n*-hexane. The crystal exhibited a photoluminescence behavior similar to that of the as-synthesized solid (Fig. 2, inset). Fig. 2a shows the PL spectrum under 340 nm light irradiation. Two groups of emission bands were found: one with an emission maximum at 439 nm and another with a maximal peak at 550 nm and two shoulder peaks. Two groups of emission also appeared in the gated PL spectrum of the crystals (Fig. 2a, red line), but the band with high energy shifted to 444 nm and became weak. The decay experiment showed two distinct emissions at 439 nm. The emission with

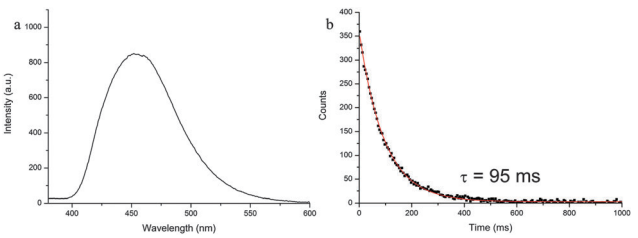

Fig. 1 Phosphorescence (PL) spectrum and decay curve of **CBA** in N_2-saturated cyclohexane at 77 K. Decay time is 0.1 ms.

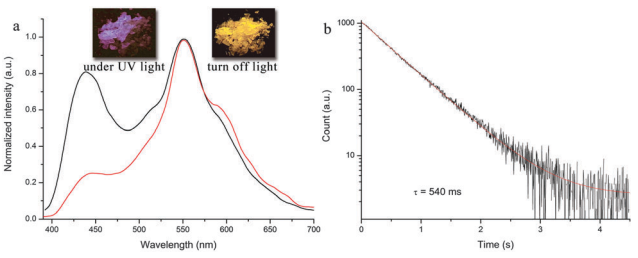

Fig. 2 (a) PL (black) and gated PL (red) spectra of **CBA** crystals and (b) decay curve of emission at 550 nm. Delay time = 0.2 ms. The excitation wavelength is 340 nm. The insets are photos of crystals under 365 nm light and then after turning off light.

a short lifetime of 1.9 ns was fluorescence, and another weak one has a long lifetime of 130 ms (Fig. S6, ESI†). Considering the similar emission wavelengths of peaks at 444 and 439 nm, we ascribed the long lifetime luminescence at 444 nm to the thermally activated delayed fluorescence (TADF) because of reverse intersystem crossing from the triplet state to the singlet state.[14] Moreover, the emission at 550 nm displayed a mono-exponential decay. The lifetime was 540 ms, and the RTP lasted for 3 s (see Movie in ESI†), suggesting that the RTP was a persistent luminescence. This result also explains why the RTP is yellow. The luminescence quantum yield reached 9%. In addition, the excitation spectrum (λ_{em} = 550 nm) has a slightly red-shifted excitation peak, implying that RTP originates from CBA, not impurity (Fig. S7, ESI†). The RTP with a longer emissive wavelength in crystals can be attributed to molecular aggregation[15] because the crystals have a red-shifted absorption peak relative to that in cyclohexane (Fig. S7, ESI†), suggesting π–π interaction between **CBA** molecules which can be supported by the crystal structure, as shown below.

To further understand the relationship between phosphorescence and intermolecular interactions, we prepared and analyzed a single crystal of **CBA**. As shown in Fig. 3, a large twisted angle (47.77°) appeared between benzaldehyde and carbazole moieties because of the steric hindrance between the hydrogen atoms of phenyl and carbazole groups. This result indicates that **CBA** is nonplanar. The carbonyl group showed two orientations and was almost coplanar with the benzene ring. In addition, molecular packing showed different types (Fig. 3b), such as dimer and crosswise packing, indicating the existence of weak exciton interaction. Such intermolecular interactions may lead to a longer emissive wavelength of RTP. Moreover, certain C–H···π interactions were found between molecules, which suppressed free molecular rotation and then activated RTP with a long persistent time.[16] The quantum chemical calculation based on the molecular structure in the crystals showed that the lowest triplet state is ascribed to HOMO → LUMO transition, and the efficient ISC from S_1 to T_3 was involved because of their different configurations (Table S5, ESI†), which allowed the RTP of crystals.

As discussed above, the crystallization of **CBA** promoted the appearance of persistent RTP because the molecular order stacking suppressed the nonradiative channels. A luminescent switch might occur if the intermolecular order packing is changed or disappeared under a mechanical force stimulus. When crystals with pink emission were ground under 365 nm light irradiation, the luminescence color firstly changed into blue. However, the luminescence color changed into purple red (PR-form) after several minutes when grinding was stopped.

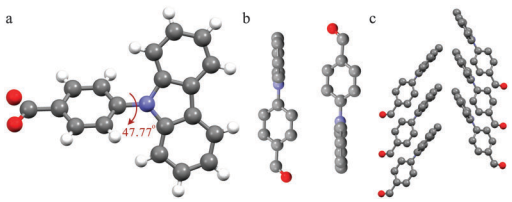

Fig. 3 (a) Molecular structure and (b) packing structures between molecules in crystals.

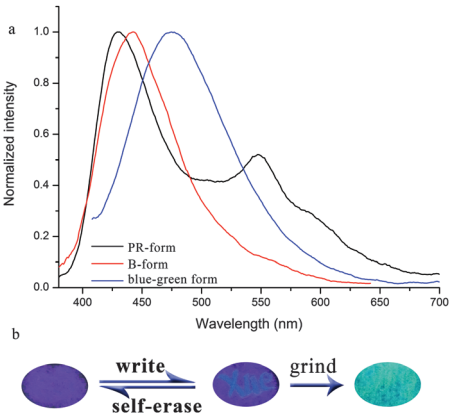

Fig. 4 (a) PL spectra of **CBA** in different states. The spectrum of only PR-form solid is gated PL spectrum. B-form powder was obtained by grinding crystals and then aging for 10 min could lead to PR-form powder. If PR-form powder on a filter paper was strongly sheared, blue-green form solid was observed. (b) Photos of ground powders, patterned film and further shearing on the surface of the filter.

The maximal emission peak of the PR-form solid located at 430 nm in the PL spectrum and a weak emission at *ca.* 550 nm could also be observed (Fig. S8, ESI†), suggesting that fluorescence is stronger than phosphorescence. Moreover, the emission band at 430 nm, ascribed to TDAF, in the gated PL spectrum also became strong, and that at 550 nm still remained but was relatively weak (Fig. 4a). A few strong diffraction peaks appeared in the XRD pattern of the **CBA** crystals. The PR-form powders possessed weak signals, but the diffraction peaks were still visible in the wide-angle region (Fig. S9, ESI†). This result suggests that the same order packing as that in crystal cells still exists after grinding and aging.[17] Hence, the emission peak at 550 nm ascribed to the phosphorescence of aggregates was strong enough so that the persistent RTP did not disappear and the duration of RTP did not shorten. However, grinding increased the amount of molecules in the unordered state. Thus, fluorescence is stronger than phosphorescence in PR-form powders and purple red luminescence is observed by the naked eye. The fact that ground powders of **CBA** still emit persistent RTP in air allows **CBA** to be applied in the anti-counterfeiting field because powders with small sizes may be easily dispersed in ink or the polymer matrix.[18]

The PR-form powders were stable at ambient temperature and could not transform into the original one with pink luminescence. Interestingly, the emissive color changed from purple red to blue again when the powders were further ground or sheared. The blue emission (B-form) peak located at 442 nm and rapidly decayed (2.7 ns, Fig. S10, ESI†), indicating its fluorescence nature. Moreover, the blue fluorescence could be rapidly restored to the original purple red one (PR-form) within 2 min, suggesting a self-healing behaviour. As discussed above, the intramolecular free rotation and vibrational motion can strongly quench the radiative transition of the lowest triplet state. Therefore, such a spectral change can be attributed to the fact that such a mechanical process yields an amorphous solid, in which the intramolecular free rotation and vibrational motion are allowed, and then phosphorescence disappears. As a result, only blue fluorescence

was visible after grinding.[16e] It is worthwhile to note that B-form powder has a longer emission wavelength relative to that of the peak at 430 nm for PR-form, which may be ascribed to molecular planarization and enhanced π–π interaction under a grinding stimulus. The rapid restoration of emission after grinding indicates that the amorphous solid is unstable and can convert into a stable crystalline state,[19] thereby inducing persistent RTP. Thus, **CBA** showed isothermally reversible phosphorescence-to-fluorescence switching in response to a mechanical stimulus. As shown in Fig. 4b, the word ''Xue'' with blue fluorescence was recorded by a stainless pin and became invisible within 1 min, implying a self-erased behavior. In addition, purple red emission switched to strong blue-green (λ_{em} = 475 nm) emission when a small amount of PR-form powder was strongly sheared on the filter paper surface. This emission was fluorescent because of its short decay time ($\langle\tau\rangle$ = 3.9 ns) and may be attributed to the hydrogen-bonded complexes of **CBA** with the hydroxyl groups on the filter surface,[20] in which the energy of T_{n,π^*} increases, being similar to that in polar solvent, and then the ISC is suppressed and fluorescence increases. Thus, a multicolor luminescent switch can be realized by simply applying a mechanical force stimulus.[21] The results obtained above indicate that the molecular phosphorescence strongly depends on the molecular packing state and intermolecular interactions. More importantly, the luminescence properties of the functional molecules with persistent RTP can be tuned by external stimuli.

In summary, a metal- and heavy atom-free nonplanar organic molecule with persistent RTP was successfully fabricated by introducing a rational carbazole moiety into a benzaldehyde matrix to produce a long-lived triplet state. More importantly, the ground powders still possess persistent RTP in air and a unique isothermally reversible phosphorescence-to-fluorescence switching property in response to a mechanical force stimulus. Hence, we believe that this work will help us to find simple organic molecules with persistent RTP features and distinctive responsive characteristics.

This work was financially supported by the National Natural Science Foundation of China (21103067 and 21374041), the Youth Science Foundation of Jilin Province (20130522134JH), the Open Project of the State Key Laboratory of Supramolecular Structure and Materials (SKLSSM2015014), and the Open Project of State Laboratory of Theoretical and Computational Chemistry (K2013-02).

Notes and references

1 (*a*) Y. Sagara and T. Kato, *Nat. Chem.*, 2009, **1**, 605–610; (*b*) Z. Chi, X. Zhang, B. Xu, X. Zhou, C. Ma, Y. Zhang, S. Liu and J. Xu, *Chem. Soc. Rev.*, 2012, **41**, 3878; (*c*) J. Wang, J. Mei, R. Hu, J. Z. Sun, A. Qin and B. Z. Tang, *J. Am. Chem. Soc.*, 2012, **134**, 9956–9966.

2 (*a*) X. Zhang, Z. Chi, Y. Zhang, S. Liu and J. Xu, *J. Mater. Chem. C*, 2013, **1**, 3376–3390; (*b*) H. Sun, S. Liu, W. Lin, K. Y. Zhang, W. Lv, X. Huang, F. Huo, H. Yang, G. Jenkins, Q. Zhao and W. Huang, *Nat. Commun.*, 2014, **5**, 3601; (*c*) A. Han, P. Du, Z. Sun, H. Wu, H. Jia, R. Zhang, Z. Liang, R. Cao and R. Eisenberg, *Inorg. Chem.*, 2014, **53**, 3338–3344; (*d*) N. Kitani, N. Kuwamura, T. Tsukuda, N. Yoshinaria and T. Konno, *Chem. Commun.*, 2014, **50**, 13529–13532; (*e*) W. A. Morris, T. Liu and C. L. Fraser, *J. Mater. Chem. C*, 2015, **3**, 352–363.

3 (*a*) M. A. El-sayed, *J. Chem. Phys.*, 1963, **38**, 2834–2838; (*b*) M. A. El-sayed, *J. Chem. Phys.*, 1963, **38**, 3032–3033.

4 S. K. Lower and M. A. El-sayed, *Chem. Rev.*, 1966, **66**, 199–241.

5 (*a*) D. R. Kearns and W. A. Case, *J. Am. Chem. Soc.*, 1966, **88**, 5087–5097; (*b*) T. Itoh, *J. Lumin.*, 2004, **109**, 221–225.

6 (*a*) Y. Wang, M. Li, Y. Zhang, J. Yang, S. Zhu, L. Sheng, X. Wang, B. Yang and S. X. Zhang, *Chem. Commun.*, 2013, **49**, 6587–6589; (*b*) Y. Dong, B. Xu, J. Zhang, X. Tan, L. Wang, J. Chen, H. Lv, S. Wen, B. Li, L. Ye, B. Zou and W. Tian, *Angew. Chem., Int. Ed.*, 2012, **51**, 10782–10785; (*c*) K. Nagura, S. Saito, H. Yusa, H. Yamawaki, H. Fujihisa, H. Sato, Y. Shimoikeda and S. Yamaguchi, *J. Am. Chem. Soc.*, 2013, **135**, 10322–10325.

7 J. Li, Y. Jiang, J. Cheng, Y. Zhang, H. Su, J. W. Y. Lam, H. H. Y. Sung, K. S. Wong, H. S. Kwok and B. Z. Tang, *Phys. Chem. Chem. Phys.*, 2015, **17**, 1134–1141.

8 X. Liu, X. Zhang, R. Lu, P. Xue, D. Xu and H. Zhou, *J. Mater. Chem*, 2011, **21**, 8756–8765.

9 M. Ren, M. Mao and Q. Song, *Chem. Commun.*, 2012, **48**, 2970–2972.

10 J. R. Lakowicz, *Principles of Fluorescence Spectroscopy*, Springer Science, New York, 3rd edn, 2006, pp.205–235.

11 (*a*) D. Lee, O. Bolton, B. C. Kim, J. H. Youk, S. Takayama and J. Kim, *J. Am. Chem. Soc.*, 2013, **135**, 6325–6329; (*b*) A. A. Lamola and G. S. Hammond, *J. Chem. Phys.*, 1965, **43**, 2129–2134.

12 N. Chattopadhyay, C. Serpa, M. M. Pereira, J. S. de Melo, L. G. Arnaut and S. J. Formosinho, *J. Phys. Chem. A*, 2001, **105**, 10025–10030.

13 (*a*) W. Wu, L. Liu, X. Cui, C. Zhang and J. Zhao, *Dalton Trans.*, 2013, **42**, 14374–14379; (*b*) G. Yong, Y. Zhang, W. She and Y. Li, *J. Mater. Chem.*, 2011, **21**, 18520–18522.

14 (*a*) H. Uoyama, K. Goushi, K. Shizu, H. Nomura and C. Adachi, *Nature*, 2012, **492**, 234–238; (*b*) D. Chaudhuri, E. Sigmund, A. Meyer, L. Röck, P. Klemm, S. Lautenschlager, A. Schmid, S. R. Yost, T. V. Voorhis, S. Bange, S. Höger and J. M. Lupton, *Angew. Chem., Int. Ed.*, 2013, **52**, 13449–13452; (*c*) L. Yao, S. Zhang, R. Wang, W. Li, F. Shen, B. Yang and Y. Ma, *Angew. Chem., Int. Ed.*, 2014, **53**, 2119–2123; (*d*) M. J. Leitl, V. A. Krylova, P. I. Djurovich, M. E. Thompson and H. Yersin, *J. Am. Chem. Soc.*, 2014, **136**, 16032–16038; (*e*) Y. J. Cho, K. S. Yook and J. Y. Lee, *Adv. Mater.*, 2014, **26**, 4050–4055.

15 (*a*) S. K. Maity, S. Bera, A. Paikar, A. Pramanika and D. Haldar, *Chem. Commun.*, 2013, **49**, 9051–9053; (*b*) R. Kabe, V. M. Lynch and P. Anzenbacher Jr., *CrystEngComm*, 2011, **13**, 5423–5427.

16 (*a*) G. He, W. T. Delgado, D. J. Schatz, C. Merten, A. Mohammadpour, L. Mayr, M. J. Ferguson, R. McDonald, A. Brown, K. Shankar and E. Rivard, *Angew. Chem., Int. Ed.*, 2014, **53**, 4587–4591; (*b*) G. Bergamini, A. Fermi, C. Botta, U. Giovanella, S. D. Motta, F. Negri, R. Peresutti, M. Gingras and P. Ceroni, *J. Mater. Chem. C*, 2013, **1**, 2717–2724; (*c*) O. Bolton, K. Lee, H. Kim, K. Y. Lin and J. Kim, *Nat. Chem.*, 2011, **3**, 205–210; (*d*) M. S. Kwon, D. Lee, S. Seo, J. Jung and J. Kim, *Angew. Chem., Int. Ed.*, 2014, **53**, 11177–11181; (*e*) O. Bolton, D. Lee, J. Jung and J. Kim, *Chem. Mater.*, 2014, **26**, 6644–6649; (*f*) H. Wang, R. X. Hu, X. Pang, H. Y. Gao and W. J. Jin, *CrystEngComm*, 2014, **16**, 7942–7948; (*g*) G. Zhang, G. M. Palmer, M. W. Dewhirst and C. L. Fraser, *Nat. Mater.*, 2009, **8**, 747–751.

17 (*a*) K. Nagura, S. Saito, H. Yusa, H. Yamawaki, H. Fujihisa, H. Sato, Y. Shimoikeda and S. Yamaguchi, *J. Am. Chem. Soc.*, 2013, **135**, 10322–10325; (*b*) L. Bu, M. Sun, D. Zhang, W. Liu, Y. Wang, M. Zheng, S. Xue and W. Yang, *J. Mater. Chem. C*, 2013, **1**, 2028–2035.

18 P. Kumar, J. Dwivedia and B. K. Gupta, *J. Mater. Chem. C*, 2014, **2**, 10468–10475.

19 (*a*) P. Xue, B. Yao, J. Sun, Q. Xu, P. Chen, Z. Zhan and R. Lu, *J. Mater. Chem. C*, 2014, **2**, 3942–3950; (*b*) N. Mizoshita, T. Tani and S. Inagaki, *Adv. Mater.*, 2012, **24**, 3350–3355.

20 E. M. Schulman and R. T. Parker, *J. Phys. Chem.*, 1977, **81**, 1932–1939.

21 (*a*) M. Teng, X. Jia, X. Chen and Y. Wei, *Angew. Chem., Int. Ed.*, 2012, **51**, 6398–6401; (*b*) Z. Ma, M. Teng, Z. Wang, S. Yang and X. Jia, *Angew. Chem., Int. Ed.*, 2012, **52**, 12268–12272; (*c*) P. Xue, P. Chen, J. Jia, Q. Xu, J. Sun, B. Yao, Z. Zhang and R. Lu, *Chem. Commun.*, 2014, **50**, 2569–2571.

